Technical Physics Letters, 2024, Vol. 50, No. 5

05.1;06.5

Growth of needle-like nanocrystals on the surface of oxidized Al and their effect in strengthening the Al-matrix composite

© *U.U. Narzulloev, M.K. Kutzhanov, I.V. Shchetinin, P.A. Loginov, D.V. Shtansky, A.T. Matveev*

National University of Science and Technology MISiS, Moscow, Russia
E-mail: matveev.at@misis.ru

Received December 18, 2023
Revised February 5, 2024
Accepted February 5, 2024

A new concept has been proposed for the creation of dispersed-strengthened composite materials (CM) due to the growth of oxide nanostructures (NS) on the surface of metal particles during the interaction of the surface oxide layer with a reaction oxide deposited on the oxidized surface of the metal particles. The concept is demonstrated using whisker-like nanocrystals (NWs) grown on the surface of oxidized Al particles. The new method ensures uniform distribution of NS on the surface of metal particles and, as a result, their uniform distribution in CM, which significantly simplifies the CM production technology. The concept covers metals with high oxygen affinity: Al, Mg, Ti, Ni, Zr.

Keywords: needle crystals, aluminum, aluminum oxide, composites, dispersion strengthening.

DOI: 10.61011/TPL.2024.05.58418.19847

Dispersed hardening is one of the main mechanisms for improving the mechanical properties of metals [1]. The highest strength characteristics of metal matrix composite materials (CM) can be obtained by using dispersed particles in the form of nanosheets or nanotubes [1]. However, nanoparticles, because of their high surface energy, are prone to agglomeration, which results in a decrease of the mechanical characteristics of CM. This paper considers a new concept of — formation of nanoparticles directly on the surface of Al particles for solving this problem. In particular, the formation of needlenanocrystals (NNCs) on the surface of Al particles due to the interaction of lithium nitrate with an aluminum oxide layer is studied.

Al powder of the grade ASD 1 with a particle size of 5–30 μm, $LiNO_3 \cdot 3H_2O$ (chemically pure) and Ar (ultra high purity) were used in this study. The Al powder was oxidized in air at 600°C for 3 h; the weight gain was 18.7%. Analysis of the powders on a scanning electron microscope JSM-7600F (JEOL, Japan) showed that the thickness of the oxide layer is approximately 300 nm. The oxidized Al was mixed with an aqueous solution of lithium nitrate (5 mass% relative to the mass of Al). The resulting powder was heated in Ar to a temperature from 700 to 1200°C and was held at this temperature for 60 min.

Scanning electron microscopy (SEM) showed that needlestructures (NS) up to 1 μm long and up to 100 nm thick were formed at 900°C; their number significantly increased, and the length increased to about 3,μm at 1000°C (Fig. 1, *a*); the surface concentration of NS is about 15 μm^{-2}; NS are not observed at a temperature below 900 and above 1100°C. The inset shows the distribution of NS in length and diameter.

X-ray images of the samples are shown in Fig. 1, *b*. Peaks corresponding to γ-Al_2O_3 (ICDD 01-074-4629) are observed after oxidation of Al. The peaks corresponding to θ-phase of Al_2O_3 (ICDD 01-080-0955) and $LiAlO_2$ (ICDD 01-075-0905) appear at 1000°C. θ-Al_2O_3 was formed during crystallization of γ-Al_2O_3. The proportion of this phase is 5.7 mass%, the proportion of lithium aluminate is 0.9 mass%.

The chemical state of the surface of the sample with needlestructure was studied by X-ray photoelectron spectroscopy (XPS) using a VersaProbeIII spectrometer (ULVAC-PHI Inc.). The spectrum of Al2*p* contains two components with binding energies (E_b) 74.0 and 75.8 eV, which correspond to Al in $LiAlO_x$ and Al_2O_3 [2]. The spectrum of O1*s* includes two components with $E_b = 531.2$ and 532.6 eV, characteristic of oxygen in Li_2O and Al_2O_3, respectively [2]. The spectrum of Li1*s* has one component with $E_b = 54.5$ eV, which corresponds to the bond Li–O in $LiAlO_x$ [2]. The results of the XPS-analysis are presented in the table. The XPS data showed the following content of elements in the sample (at.%): Li — 20.75, Al — 27.47, O — 50.56, N — 1.22; the phase composition of the sample surface corresponds to the phase content (mol.%): $LiAlO_2$ — 85.2, Al_2O_3 — 12.3, AlN — 2.5.

Figure 2 shows the results of transmission electron microscopy (TEM). Two types of needlestructures are observed: amorphous (diameter 2–40 nm) and crystalline (diameter 40–100 nm). The distances between the projections of atomic planes are 0.29–0.31 nm on high-resolution TEM images (Fig. 2, *c*) showed. Such interplane distances are observed in $Li_2O{\cdot}Al_2O_3$, γ-Al_2O_3 and δ^*-Al_2O_3. The electron diffraction pattern (Fig. 2, *b*) acquired from the needlestructure contains point reflexes corresponding to the interplane distances 0.275, 0.245 and 0.222 nm, which are also observed in the listed phases.

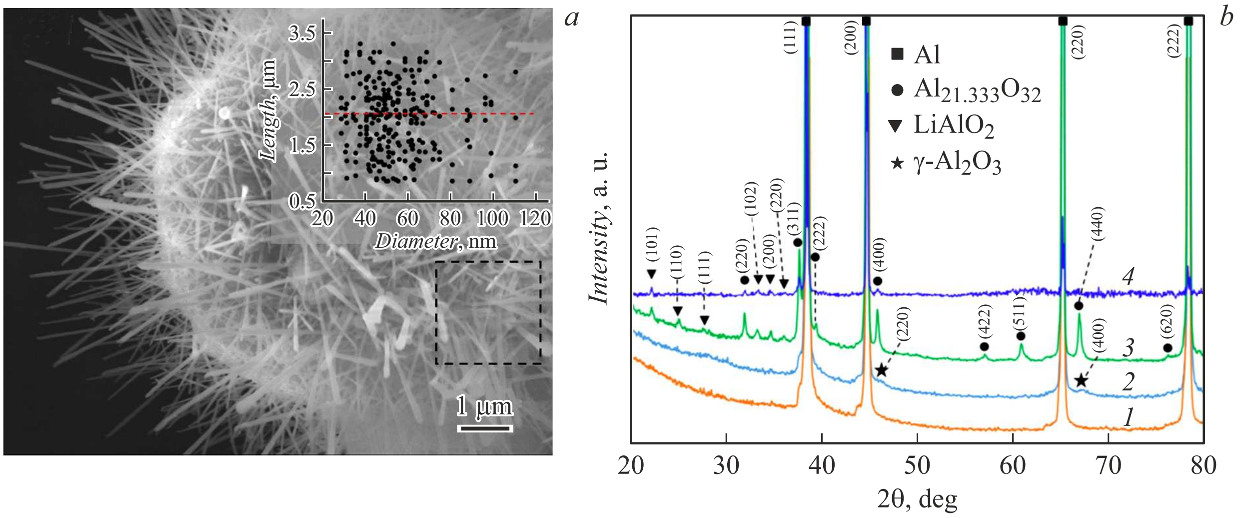

Figure 1. *a* —SEM image of an Al sample with needlestructures after high-temperature annealing for 60 min at 1000°C. The inset shows the distribution of NS in length and diameter. *b* — the X-ray images of Al samples: initial sample (*1*), oxidized sample (*2*), after high-temperature annealing (*3*), as well as Al/$LiAlO_2$ composite (*4*).

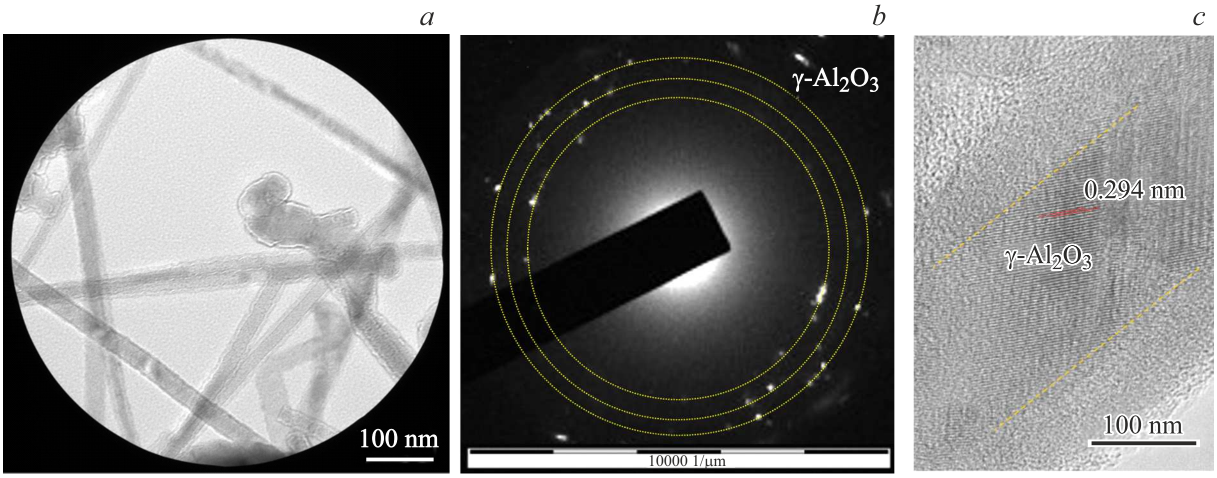

Figure 2. *a* —the TEM-image of needle structures; *b* — the electron diffraction from the same region; *c* — high-resolution TEM-image of one needlestructure.

The bond energies E_b and fractions υ of the component in the X-ray photoelectron spectra of a sample with a needlestructure

Line	$LiAlO_2$		Chemical bond
	E_b, eV	υ, %	
O1*s*	531.2 532.6	85.11 14.89	Li$-$$O_x$$-$Al Al$-$$O_x$
Al2*p*	74.0 75.8	80.63 19.37	Li$-$Al$-$$O_x$ Al$-$$O_x$
Li1*s*	54.5	100.00	Li$-$$O_x$

These results indicate that needlestructures are the needlenanocrystals of aluminum oxide and/or lithium aluminate. There is no - crystallographic orientation between the needlenanocrystals and the particle on which they grew. It should be noted that the diameter of the needlenanocrystals remains constant along their length, while spherical nanoparticles of catalysts at their vertices are not observed, which are characteristic of the growth of needlenanocrystals based on the vapor–liquid–crystal mechanism [3–8]. The aluminum is in a liquid state and is retained by an oxide shell at 900–1000°C. It can be assumed that the growth of needlenanocrystals is associated with the constant supply of aluminum and its suboxides (formed by the interaction of the aluminum melt with the inner surface of the oxide shell) by diffusion through the defects of the oxide layer under the impact of positive pressure inside the particles caused by the difference of the coefficients of thermal expansion of liquid aluminum and the oxide shell.

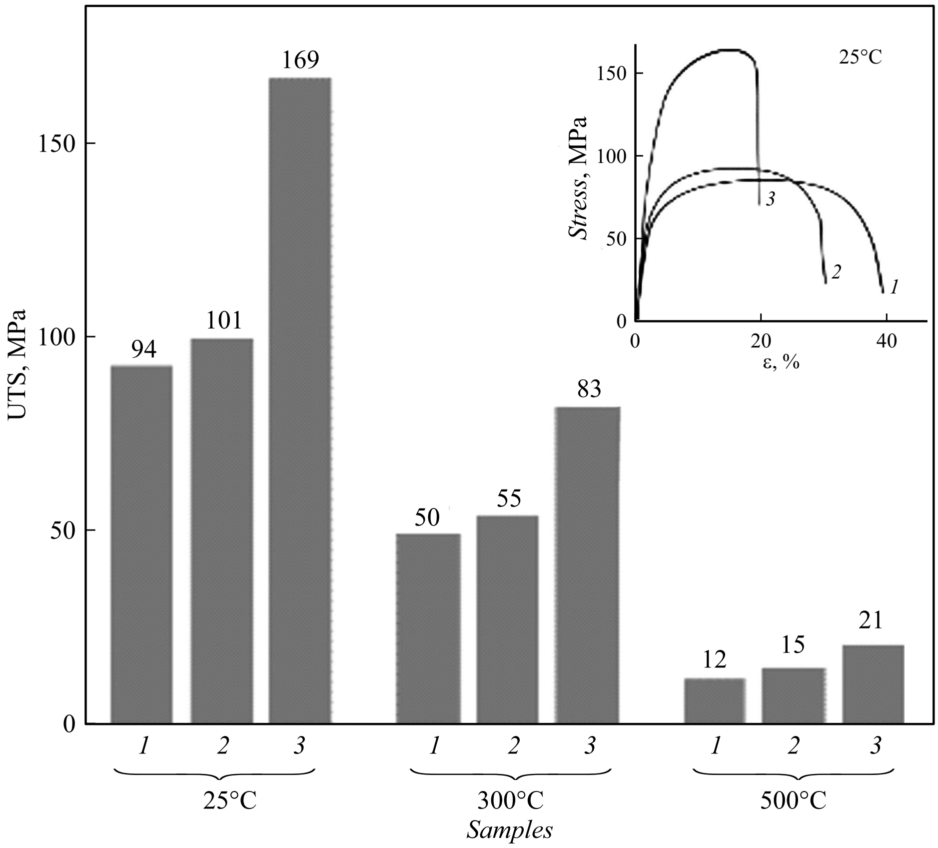

Figure 3. Ultimate tensile strength (UTS) of Al samples: initial sample (*1*), oxidized sample (*2*) and sample with needlenanocrystals (*3*). The deformation curves of the specified samples at 25°C are shown in the insert.

Composite material was obtained from a material containing needle nanocrystals by spark plasma sintering using Labox 650 SPS unit system (Sinter Land Inc., Japan): sintering temperature 630°C, vacuum, compression pressure 35 kN, sintering time 10 min. The Vickers hardness was determined using DuraScan 70 hardness tester (EMCO-TEST, Germany), tensile strength was determined using Shimadzu AG-Xplus 20 kN testing machine (Shimadzu Corp., Japan). Fig. 3 shows tensile strength of the samples of the initial Al (*1*), oxidized Al (*2*) and Al with needle nanocrystals (*3*). The deformation curves of these samples at 25°C are shown in the insert. The strength of a sample with 0.9 mass% of $LiAlO_2$ increased by 67% at 25°C, and the hardness increased by 64% (from 28 to 50 HV_1). A significant increase in strength and hardness can be expected with an increase of the amount of needle nanocrystals [1,9].

Thus, a method for obtaining Al_2O_3 and $LiAlO_2$ needle nanocrystals with diameters from 30 to 120 nm and lengths up to 3 μm on the surface of Al particles was developed. The uniform distribution of needle nanocrystals on the surface of Al particles ensures their uniform distribution in the composite material matrix, which simplifies the technology of production of composite materials, since it eliminates the stage of ball grinding of powder mixtures. A new concept was proposed for the creation of dispersed-hardened metals through the growth of oxide nanostructures on the surface of metal particles. The concept covers a broad range of metals with a fairly high affinity for oxygen.

Funding

This study was carried out as part of project No. 22-29-01103 of the Russian Science Foundation.

Conflict of interest

The authors declare that they have no conflict of interest.

References

[1] W. Abd-Elaziem, M. Khedr, A.H. Elsheikh, J. Liu, Y. Zeng, T.A. Sebae, M.A. Abd El-Baky, M.A. Darwish, W.M. Daoush, X. Li, Eng. Fail. Anal., **155**, 107751 (2024). DOI: 10.1016/j.engfailanal.2023.107751

[2] S. Maiti, H. Sclar, R. Sharma, N. Vishkin, M. Fayena-Greenstein, J. Grinblat, M. Talianker, L. Burstein, N. Solomatin, O. Tiurin, Y. Ein-Eli, M. Noked, B. Markovsky, D. Aurbach, Adv. Funct. Mater., **31**, 2008083 (2021). DOI: 10.1002/adfm.202008083

[3] E.I. Givargizov, A.A. Chernov, Kristallografiya, **18** (1), 147 (1973) (in Russian).

[4] V.G. Dubrovskii, N.V. Sibirev, G.E. Cirlin, Tech. Phys. Lett., **30** (8), 682 (2004). DOI: 10.1134/1.1792313.

[5] V.G. Dubrovskii, G.E. Cirlin, I.P. Soshnikov, A.A. Tonkikh, N.V. Sibirev, Yu.B. Samsonenko, V.M. Ustinov, Phys. Rev. B, **71**, 205325 (2005). DOI: 10.1103/PhysRevB.71.205325

[6] G.E. Cirlin, V.G. Dubrovskii, N.V. Sibirev, I.P. Soshnikov, Yu.B. Samsonenko, A.A. Tonkikh, V.M. Ustinov, Semiconductors, **39** (5), 557 (2005). DOI: 10.1134/1.1923565.

[7] N.V. Sibirev, Y.S. Berdnikov, I.V. Shtrom, E.V. Ubyivovk, R.R. Reznik, G.E. Cirlin, Tech. Phys. Lett., **48** (2), 26 (2022). DOI: 10.21883/TPL.2022.02.52841.18869.

[8] S.A. Ammer, V.S. Postnikov, *Nitevidnye kristally* (Voronezh. politekhn. in-t, Voronezh, 1974) (in Russian).

[9] M.K. Kutzhanov, A.T. Matveev, A.V. Bondarev, I.V. Shchetinin, A.S. Konopatsky, D.V. Shtansky, Metals, **13**, 1696 (2023). DOI: 10.3390/met13101696

Translated by A.Akhtyamov